ORIGINAL RESEARCH

Screening of the Medicinal Plant-Based Metabolites Responsible for Silver Nanoparticle Phytofabrication

Article history:
Received: 22-12-2023
Revised: 09-04-2024
Accepted: 11-05-2024
Published: 02-07-2024

Preeti Sharma[a], Basudha Sharma[b]

Abstract: In this study, the detailed phytochemical composition of two medicinal plants was investigated and their importance in silver nanoparticles (AgNPs) synthesis was highlighted. Aqueous extracts from the leaves of both plants were used for various analytical techniques, including UV-vis spectroscopy, Gas chromatography-mass spectrometry (GC-MS), Fourier transform infrared spectroscopy (FTIR) and Thin layer chromatography (TLC). Quantification of total phenolics and flavonoids in different fractions of plant extracts revealed significant concentrations. TLC profiling showed a higher abundance of free phenolic and flavonoid compounds compared to bound forms in both plants, suggesting that they contribute significantly to total phenolic and flavonoid content. UV-vis spectra from 200 to 600 nm revealed the presence of aromatic rings and chromophores in leaf extracts. Furthermore, the GC-MS analysis identified several bioactive compounds, some of which were found to be common between these two species. The results demonstrate that various bioactive compounds such as phenols, flavonoids, alkaloids, carotenoids and terpenoids were present in these plant species. These compounds efficiently serve as both reducing and stabilizing agents during phytofabrication of AgNPs, consequently eliminating the need for the use of hazardous chemicals.

Keywords: Profiling; Phenolic; Gas chromatography; Nanoparticles.

1. INTRODUCTION

Nanotechnology, a frontier in applied science, has created a solid foundation for industrial revolution and transformation in numerous sectors such as healthcare, agriculture, food, environment, information science, etc. Due to its unique qualities, it offers substantial participation from household to corporate sectors (Bachheti *et al.*, 2022). The properties of the nanoparticles that are lacking in their bulk counterparts include size, surface area to volume ratio, charge and shape. These properties also determine its reactivity, conductivity, solubility, emission, absorption and optical behavior, which can be modified by changing the various reaction parameters during the synthesis of nanoparticles (Koul *et al.*, 2018). These remarkable properties and functions of nanomaterials can be achieved by using physical, chemical and biological approaches (Ahsan *et al.*, 2023). However, the focus of researchers has currently shifted towards biological methods rather than physical and chemical due to their environmental friendliness, cost-effectiveness, energy efficiency, and avoidance of toxic chemicals (Ijaz *et al.*, 2020). Among all biological entities (bacteria, algae, fungi, plants, etc.), medicinal plants are abundant natural resources with a

[a] Department of Botany, M.M. College Modinagar, Ghaziabad Uttar Pradesh 201201, India.
[b] Department of Botany, M.M. College Modinagar, Ghaziabad Uttar Pradesh 201201, India. Corresponding author: basudhammc@gmail.com

variety of phytochemical components. Unlike microbial resources, which often require complicated and multi-step processes, medicinal plants offer the advantage of easy handling from nanoparticle synthesis to scale-up (Sanjivkumar *et al.,* 2023). Medicinal plants have an abundance of small and complex metabolites (phenols, flavonoids, alkaloids, quinones, terpenoids, tannins, lectins, coumarin, saponin, etc.) in their roots, stems, bark, leaves, shoots, flowers and nuts (Saranraj *et al*., 2023). These phytochemicals are used in traditional, indigenous and modern medicines to treat numerous diseases and are supposed to have the ability of reduction, and stabilization during nanoparticle synthesis. The crucial role of phytometabolites in a plant's overall metabolism determines whether they are classified as primary or secondary compounds (Bachheti *et al.,* 2023 Chandra *et al.,* 2022). Phenolic compounds contain hydroxyl group directly linked to an aromatic ring which can donate a proton (H+) under certain conditions, making them important in various fields (Dai *et al.,* 2010). Alkaloids often contain basic nitrogen atoms synthesized from amino acids, such as tyrosine, which serve as defensive agents in plants (Umashankar *et al.,* 2020). Other secondary metabolites, such as saponins play a role as surfactant glycosides, whereas carotenoids and terpenoids contribute to the aroma, taste and color of plants (Alzandi *et al*., 2010). Therefore, plant extracts contain several compounds and functional groups that are supposed to play a crucial role in reacting with precursor compounds to form nanoparticles. For instance, the hydroxyl group of eugenols in clove extracts serves as a reducing agent in silver nanoparticle synthesis, while terpenoids serve as stabilizing agents. In contrast, terpenoids in chamomile flower extracts *(Matricaria chamomilla)* act as reducing and stabilizing agents in the nanosilver formation (Parlinska-Wojtan *et al.,* 2016). Proteins present in *Calendula officinalis* leaf extracts play a crucial role in the reduction, capping and stabilization of nanoparticles from silver (El-Kemary *et al.,* 2016). Similarly, quercetin and flavonoids reduced silver nitrate precursor in an alkaline medium and exhibited various therapeutic properties. Several other studies indicated the role of quercetin, flavonoids, tannin, terpenoids in nanoparticle synthesis (Durran *et al.,* 2015; Hussain *et al.,* 2016). Understanding these phytochemicals derived from medicinal plants is necessary so that specific nanoparticles with the desired properties can be produced from these phytometabolites.

In light of these historical uses and medicinal properties, the current study was designed for comprehensive analysis of the phytochemical composition of *Acokanthera oppositifolia* and *Leucaena leucocephala* and to determinethe role of these phytometabolites in the synthesis of silver nanoparticles. The rationale behind selecting *Acokanthera oppositifolia* and *Leucaena leucocephala* for this study is due to their extensive historical use as remedies for a variety of diseases, which suggests the presence of various bioactive compounds with potential medicinal properties. These plants are abundant in nature and easily accessible, facilitating experimentation and scalability of nanoparticle synthesis processes. *Acokanthera oppositifolia,* a member of the Apocynacea family, is known for its traditional use in the treatment of snakebites, spider bites, syphilis, headaches and stomachaches, colds, abdominal pain, cramps, measles and tapeworm infestations (Parry, 2007; Adedapo *et al.,* 2008). The roots of this plant, in powder form, serve as an oral remedy for pain and snakebites, while root decoctions are effective against anthrax and tapeworm infestations (Watt & Breyer-Brandwijk, 1962). In addition, a decoction of boiling leaves relieves heart water diseases in sheep (Dold & Cocks, 2001). Cardiac glycosides are used in the treatment of heart failure and demonstrate their therapeutic versatility (Krishna *et al.,* 2015). Despite its toxicity, the pulp of the ripe fruit is edible and enjoyed by birds and animals. Similarly, the "miracle tree" *Leucaena leucocephala,* which belongs to the Fabaceae family, has countless medicinal uses in various cultures as traditional medicine. Its roots, stems, leaves, flowers and fruits are used to prepare antidotes to poisons and to relieve pain from snake bites (Deshmukh *et al.,* 2018). The root and bark are used in decoctions to prevent miscarriage (DeFilipps & Krupnick, 2018). The warming properties of the leaves stimulate blood circulation and help regulate gastrointestinal functions. Due to their skin-friendly properties, they are also extremely effective in the treatment of Grade II burns (Kurnia *et al.,* 2019). The seeds are known for their anthelmintic effects and relieve ailments such as insomnia, swelling, kidney inflammation and diabetes (Umboro & Hamdani, 2019). While previous studies have extensively investigated the medicinal properties and phytochemical profiles of various plant species, limited attention has been given to elucidating the role of these metabolites in the synthesis of silver nanoparticles.

Furthermore, the unique synthesis capabilities of *A. oppositifolia* and *L. leucocephala* have not been thoroughly explored in prior research. The current approach involves the use of multiple analytical techniques, including UV-vis spectroscopy Gas chromatography-mass spectrometry (GCMS), and Fourier transform infrared spectroscopy (FTIR) were used. Furthermore, Thin-layer chromatography (TLC) was used to characterize the open and free phytochemicals present in the extracts. This comprehensive analysis provides valuable insights into the specific compounds and functional groups involved in AgNPs synthesis, thus paving the way for more targeted and efficient green synthesis approaches. This contribution is essential for the further development of scientific knowledge at the interface between plant research and nanotechnology.

2. MATERIAL AND METHOD

2.1. Chemical and Reagents

The silver nitrate salt ($AgNO_3$), toluene, ethyl acetate, formic acid, methanol, and acetic acid were purchased from Sigma-Aldrich. The following items were purchased from E-Merck India: gallic acid, quercetin ferric chloride ($FeCl_3$), sodium hydroxide (NaOH), Folin-Ciocalteu reagent (FCR), aluminum chloride ($AlCl_3$), sodium carbonate (Na_2CO_3) and sodium nitrite (NaNO2).

2.2. Collection of plant leaves and extraction of metabolites

The leaves of plants were collected from Multanimal Modi College, Modinagar and confirmed by experts from the botany department. After thoroughly washing with double distilled water subjected to shadow drying and crushed into powder form. The powder was extracted using a Soxhlet followed by condensation of the filtrate under a vacuum utilizing by rotary evaporator at 40 °C. Further, this aqueous extract was used as a total fraction for all analytical methods. Meanwhile, to obtain free phytochemicals, powder was extracted with water after being homogenized and filtrate extracts were dried on a rotary evaporator. For the isolation of bound phytochemicals, the free-extraction residues were dried and subjected to alkaline hydrolysis to be acidified, and the supernatant was extracted and concentrated four times with ethyl acetate. These free and bound phytochemical fractions were collected and used for the quantification of phenolics, flavonoids, and TLC analysis (Su *et al.*, 2014).

2.3. Quantification of total phenolics and flavonoids

Various reliable color intensity-based methods were used for the preliminary phytochemical analysis of phenols, flavonoids, alkaloids, saponins and tannins as given in Table 1. In the secondary stage, Folin-Ciocalteu reduction and aluminum chloride-based approach were used to estimate the total amount of phenol and flavonoid, respectively. By combining 0.1 ml of each fraction of extracts with 0.5 ml of diluted Fc reagent and then adding 20% Na_2CO_3. After an incubation period of 2 hours, the final reaction volume was adjusted to 10 ml with water and absorbance was measured at 765 nm to determine the phenol content (Yu *et al.*, 2002; Sharma *et al.*, 2015). To determine the flavonoids 0.3 ml of both $AlCl_3$ (10%) and sodium nitrite (5%) were combined with 1 ml of each fraction. After 5 minutes, 2 ml (1 M) NaOH was added and diluted with 8.4 ml water and the absorbance was recorded at 510 nm. The quantity of total phenolics and flavonoids was calculated as mg of standard/ gram dry weight of plant sample (g DW), where gallic acid and quercetin were used as a standard for phenolics and flavonoids. Each experiment was performed in triplicate (Kim *et al.*, 2003).

2.4. Thin-layer Chromatography Analysis

TLC was employed to separate and visualize distinct components within plant extracts by observing their migration distances and characteristic spots on the TLC plate. Each fraction of plant extracts (free, bound, total) at 1 mg/ml concentration was transferred onto a TLC plate, (Kieselgel 60 F254) purchased from Merck India, Mumbai. After loading the samples, these plates were placed in two different mobile phases (A), toluene: ethyl acetate: methanol: formic acid (9:3:1:0.6) and mobile phases (B), ethyl acetate: water: formic acid: acetic acid (10:3:1:1). The resulting spots were then observed under visible and UV light at 254 and 365 nm wavelength before and after the (derivatization) treatment with 1% $FeCl_3$ spray. The relative frequency (Rf) was calculated by measuring the migrated distance of the spot (Lalrinzuali *et al.*, 2015; Nistane *et al.*, 2019).

S.No.	Phytochemicals	Procedure	Observation	Reference
1.	Phenols	Sample + 0.5 ml (2%) $FeCl_3$	Appearance of blue or green colour	(Tepal, 2016)
2.	Flavonoids	Sample + Few drops of 1% NaOH followed by a few drops of 1% HCl	Intense yellow color appeared, which subsequently disappeared	(Hossain *et al.,* 2013)
3.	Alkaloids	Sample + 2% H_2SO_4 + Wagner's reagent	Formation of reddish-brown precipitate	(Kancherla *et al.,* 2020)
4.	Saponin	Sample + 0.5 ml of distilled water + Shaken	Layer of foam formed on the top	(Harborne, 2020)
5.	Tanins	Aqueous extracts + diluted with chloroform and acetic anhydride (1 ml each) + sulfuric acid (1 ml)	Formation of green colour	(Harborne, 2020)

Table 1. Method of Preliminary Phytochemical Analysis using different chemical reagents.

2.5. Uv-visible and FTIR pectroscopy Analysis

To characterize and evaluate the optical behavior, particularly the light absorption in the UV-vis spectrum of the phytometabolites, UV-vis spectroscopy was used (Lalrinzuali *et al.*, 2015). The absorption was measured in a range of 200 to 800 nm by a double-beam UV-vis spectrophotometer (Labtronics model LT-2201). UV-vis spectrometric analysis was performed by preparing a solution with a concentration of 1 mg/ml. This was achieved by mixing 1 mg of the extracted powder obtained using a Soxhlet extractor with 1 ml of distilled water. Subsequently, 3 ml of this prepared sample was added to the cuvette for analysis. The functional groups present within the phytometabolites of both plant extracts were determined by FTIR with NicoletTM - IS-50 FTIR (Thermo Scientific) using the process of KBr pellet technique, covering the range of 4000-500 cm^{-1} by the attenuated total reflection (ATR) method in transmission mode. After centrifugation at 3000 rpm for 10 minutes, the aqueous extracts were filtered through Whatman No. 1 filter paper, and the resulting dry powder was used for FTIR analysis (Gururaja *et al.*, 2016; Vanitha *et al.*, 2019).

2.6. GC-MS Spectrum Analysis

Gas chromatography-mass spectrometry (GC-MS) analysis was performed by Agilent 8890/5977B series, (Agilent 5977B EI/CI MSD) model with an electron multiplier (EM) autosampler. Series II three-axis detectors with high-energy dynodes and electron multipliers were used for detection. Helium was used as a carrier gas at 1 ml/min flow rate. The injecting volume was 2 µl and maintained at 280 °C. Temperature was increased from 40 to 280 °C, with an isothermal period lasting 5 minutes. Identification of phytometabolites was achieved by evaluating the retention time, MS fragment generated and identifying the percentage of the phytometabolites from the total peak area. Interpretation of phytometabolites was identified by their retention time and comparison with compounds available in the NIST20 library (Gomathi *et al.*, 2015; Vanitha *et al.*, 2019).

2.7. Phytofabrication of Silver Nanoparticle

The plant extract powder 2 grams was dissolved in 100 ml of water and heated at 60 °C for one hour. For silver nanoparticle fabrications silver nitrate (25 mM) mixed with plant aqueous extract (2 g/100 ml) in 5:1 ratio and characterized by UV-vis spectroscopy, Transmission electron microscopy (TEM), X-ray diffraction (XRD), energy dispersive analysis (EDAX), and Fourier transformer infrared spectroscopy (FTIR), as detailed previously reported (Sharma *et al.*, 2023).

3. RESULTS AND DISCUSSION

3.1. Phenolics and Flavonoids Contents in Different Fractions

Qualitative analysis exhibited phenols, flavonoids and tannin present in both plants. However, alkaloids were exclusively detected in *L. leucocephala*, whereas saponins were absent in both plant species

depicted in Table 2. All fractions of both samples contained significant amounts of phenolics and flavonoids, with higher concentrations found in the total fraction in comparison to free and bound fractions. The phenolic values of *L. leucocephala* were 2.84, 1.79 and 1.05 mg GAE/g DW for total, free and bound samples, respectively. In contrast, *A. oppositifolia* showed higher phenolic levels at 12.06, 8.4, and 3.6 mg GAE/g DW in the total, free, and bound fractions, respectively. However, the flavonoids in *L. leucocephala* were 3.50, 2.30 and 1.20 mg QE/g DW in the total, free and bound fractions, respectively. While, *A. oppositifolia* showed slightly lower flavonoid levels in the total, free and bound samples at 2.9, 1.8 and 1.1 mg QE/g DW. Phenolic contents were more in *A. oppositifolia*, while flavonoids were more in *L. leucocephala* as illustrated in Fig. 1.

	A. oppositifolia	***L. leucocephala***
Phenol	+	+
Alkaloids	–	+
Flavonoids	+	+
Saponin	–	–
Tannin	+	+

Table 2: Qualitative screening profile of phytometabolites in plant extracts.

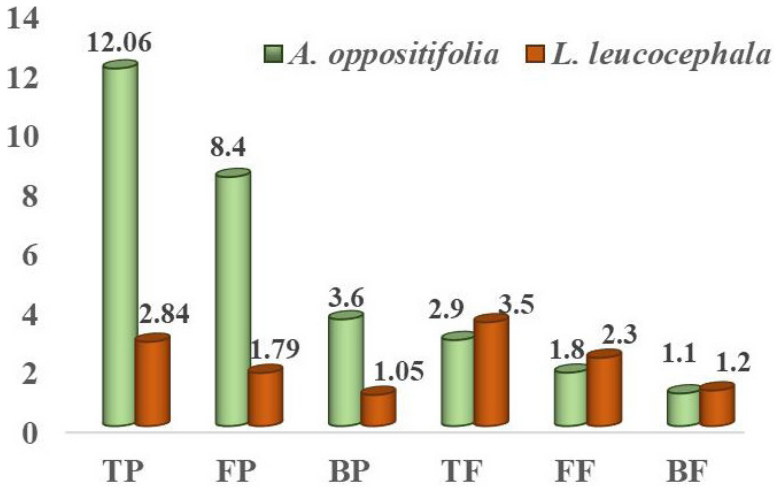

Figure 1. Quantitative analysis of phenolic and flavonoids in Total, Free, and Bound fractions of plant extracts.

3.2. TLC profiling

TLC profiling in Table 3 exhibited different Rf values ranging from 0.23 to 0.88 and 0.28 to 0.92 for *A. oppositifolia* and *L. leucocephala*, indicating different compounds within different fractions (free, bound, and total) and conditions (normal, after spraying) with two mobile phases (A and B). Mobile Phase A under normal conditions, *A. oppositifolia* displayed distinct spots for free (Rf = 0.61), bound (Rf = 0.55), and total (Rf = 0.46), appearing as light to dark green. Meanwhile, *L. leucocephala* exhibited 3 spots for the free fraction from yellow, dark yellow, and green (Rf = 0.55, 0.70, 0.90), one spot for the total fraction. After spray treatment, both extracts showed notable changes in spot coloration and Rf values. *A. oppositifolia* exhibited two spots of black and light green in free, one for bound and two for total fraction, each with varying Rf values. while *L. leucocephala* spots transitioned into varying shades of light and dark green, displaying different ranges of Rf values with four, one, and one spot in the free, bound, and total fraction of the sample. In Mobile Phase B under normal conditions, *A. oppositifolia* indicated no visible spots for the free and bound fraction, but one light green spot (Rf = 0.86) for the total fraction was observed. Conversely, *L. leucocephala* exhibited dark brown spots for free (Rf = 0.41) and a light brown spot (Rf = 0.48) for the total fraction. But after spray treatment, the maximum number of spots observed in *L. leucocephala* was two, two, and three for free bound and total fraction, respectively, with a range of colors (gray, purple, and dark green) with different Rf values. *A. oppositifolia* displayed deep black spots (Rf = 0.86) in free and one light black and one dark green in total fraction.

For *A. oppositifolia*, the total fraction showed the most spots (2) compared to free and bound fractions using both mobile phases (A and B). The bound fraction had minimal or no distinct spots. However, in *L. leucocephala*, the free fraction showed the most spots (4) compared to the total and bound fractions with both mobile phases. The bound fraction consistently had the fewest spots and only showed one spot after spraying in mobile phase A. Mobile phase A yielded the highest number of spots for *A. oppositifolia*, while *L. leucocephala* had around similar spot distributions for both mobile phases. The Rf values observed for the standards were 0.38, 0.53, and 0.61, corresponding to caffeic acid, coumaric acid, and cinnamic acid, used as phenolic standards. Quercetin, rutin, and naringin exhibited Rf values of 0.53, 0.93, and 0.73 used as standards for flavonoids. Multiple bands were observed within this range during the analysis. The Rf value of 0.53 in the free fraction of *A. oppositifolia* indicated caffeic acid and coumaric acid presence. Furthermore, in *A. oppositifolia* at Rf 0.53, evidence of quercetin was observed in the free fraction. For *L. leucocephala*, bands at Rf 0.55, 0.70 and 0.90 were detected in the free fraction.

	***A. oppositifolia* Spots (Rf)**			***L. leucocephala* Spots (Rf)**		
	Free	**Bound**	**Total**	**Free**	**Bound**	**Total**
Mobile Phase A						
Normal	1Light green (0.61)	1Light green (0.55)	1Dark green (0.46)	1Yellow (0.55)	No visible	1Light yellow (0.69)
			1Light yellow (0.76)	1Dark yellow (0.70)		
				1Light green (0.90)		
After spray	1Black (0.30)	1Light green (0.23)	1Light black (0.38)	1Light black (0.30)	1Light green (0.30)	1Dark green (0.92)
	1Light green (0.53)		1Black (0.50)	1Light green (0.51)		
				1Light black (0.76)		
Mobile Phase B				1Dark black (0.84)		
Normal	No visible	No Visible	1Light Green (0.86)	1Dark brown (0.41)	No visible	1Light brown (0.48)
After spray	1Deep black (0.86)	No visible	1Light black (0.39)	1Gary (0.56)	1Purple (0.41)	1Dark green (0.28)
			1Dark Green (0.88)	1Dark yellow (0.96)	1Light spray (0.86)	1Gray (0.48)
						1Light green (0.86)

Table 3. TLC analysis in different fractions of plant extracts with the number of spots and their (Rf) values within this range during the analysis.

These Rf values indicated the presence of quercetin, rutin, and naringin, respectively, in the free fraction of *L. leucocephala.* The predominance of free phenolic and flavonoid compounds compared to their bound counterparts suggests that these were main contributors in the total phenolic and flavonoid contents in both plants. This highlights the essential involvement of free compounds in shaping the phytochemical composition of plants.Similar to previous finding that free phenolics were main contributors in different biological activities compared to bound (Min *et al.*, 2012; Zhu *et al.*, 2019). The TLC plates for both the solvent systems are shown in Fig. 2 (i, ii). These transformations in color suggest potential chemical reactions or interactions within the compounds present in the extracts under different chromatographic conditions. The TLC results are consistent with the findings of UV and FTIR, indicating the presence of quercetin, rutin, and naringin in the free fraction of *L. leucocephala*, while in *A. oppositifolia*, caffeic acid, coumaric acid, and quercetin were observed.

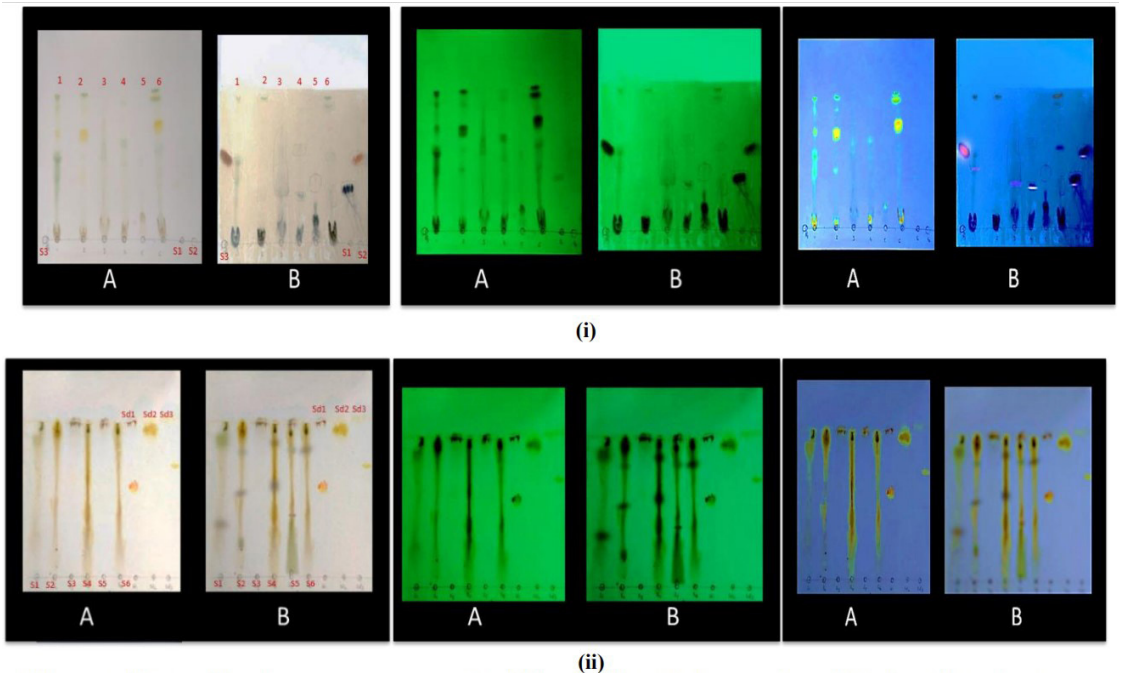

Figure 2. TLC profile of aqueous extracts under different light; (A) in normal and (B) after derivatization (i) *A. oppositifolia* and (ii) *L. leucocephala.*

3.3. UV-vis Spectrum

The UV-vis spectra ranging from 200 to 600 nm were used to detect aromatic rings and chromophores in leaf extracts, which exhibited distinct peaks and a well-defined baseline due to electronic transitions of π-bonds, σ-bonds and lone pairs of the phytochemicals present in the extracts (Mabasa *et al.*, 2021). The UV-vis spectra showed various peaks in the approximate range of 216 to 455 nm with absorptions ranging from 0.02 to 0.40 absorption units, depicted in Fig. 3a,c. Peaks ranging from 234 to 676 nm are associated with presence of phytometabolites like alkaloids, phenols, and flavonoids, as previously reported (Patle *et al.*, 2020). The majority of peaks observed in this wavelength range, as reported in Table 4, strongly indicate the presence of these metabolites in the plant extracts. The presence of phenols and their derivatives was indicated by peaks at 282, 317 and 284, 313 nm in *A. oppositifolia* and *L. leucocephala.* Peaks at 219, 297, 246 and 327 nm, detected exclusively in *L. leucocephala*, indicate the presence of caffeic acid. Both plants exhibit peaks similar to those of chlorogenic acid, protocatechuic acid, p-coumaric acid and ferulic acid as previously reported, supporting the presence of these metabolites (Patle *et al.*, 2020). However, the absence of the second peak (322 nm) for ferulic acid in *L. leucocephala* could be due to possible overlapping signals from other compounds that could obscure or hide the peak. Peaks observed at specific wavelengths (305, 317, 329 nm and 241, 245, 257 nm) in *A. oppositifolia* and peaks at 305, 246 and 284 nm in *L. leucocephala* support the presence of flavonoids as characteristic bands of flavonoids like Band I (300-400 nm) and Band II (240-280 nm) (Belay *et al.*, 2009; Saxena *et al.*, 2012). The differences in the absorption peaks of these plants indicate possible variations in the composition of the compounds and highlight the inherent chemical diversity of these species. The phytometabolites identified in Table 4, play a crucial role in reducing silver ions and stabilizing nanoparticles due to their diverse functional groups, including carboxyl, hydroxyl, ortho-dihydroxy, amino, and catechol, enhancing their reducing and stabilizing properties (Edreva *et al.*, 2008). These natural antioxidants, rich in hydroxyl and carboxyl groups, effectively reduce Ag ions to AgNPs during synthesis, while their conjugated double bonds augment their reducing capacity.Caffeic acid's hydroxyl and carboxyl groups facilitate interaction with silver ions, aiding in AgNPs reduction and potential stabilization (Nilsson *et al.*, 2008). Cinnamic acid's high oxidation tendency enables it to reduce and stabilize AgNPs under alkaline conditions (Wang *et al.*, 2006).

Phytochemical Compound	Absorption Maxima	*A. oppositifolia*		*L. leucocephala*		Ref.
		Wavelength (nm)	Abs. (a.u.)	Wavelength (nm)	Abs. (a.u.)	
Phenol and their derivatives	280, 320	282, 317	0.06, 0.08	284, 313	0.06, 0.05	(Mabasa *et al.,* 2021)
Caffeic acid	220, 295,325	—	—	219,246, 297, 327	0.2, 0.03, 0.24	(Mabasa *et al.,* 2021)
Chlorogenic Acid	217, 324	216, 329	0.40, 0.23	219, 327	0.2, 0.24	(Patle *et al.,* 2020)
Protocatechuic Acid	224, 258, 294	222, 257, 292	0.31,0.08, 0.06	257, 297	0.05, 0.03	(Patle *et al.,* 2020)
Coumaric Acid	228, 308	228, 305	0.25, 0.07	228, 307	0.26, 0.05	(Patle *et al.,* 2020)
Ferulic Acid	233, 322	232, 329	0.28, 0.23	232	0.29	(Patle *et al.,* 2020)
Flavonoids (Band I)	300-400	305, 317, 329	0.07, 0.08, 0.23	305	0.04	(Belay *et al.,* 2009)
Flavonoids (Band II)	240-280	241, 245, 257	0.40, 0.22, 0.08	246, 284	0.32, 0.06	(Belay *et al.,* 2009)
Carotenoids	400-450	412, 430	0.11, 0.11	412, 430	0.07, 0.07	(Kowalski *et al.,* 2005)
Terpenoids	400-550	455	0.08	452	0.05	(Patle *et al.,* 2020)

Table 4. Peak values of the UV-vis spectra of plant extracts with their corresponding phytometabolites.

Additionally, the reducing capacity of phenolic acids, correlated with their hydroxyl groups, promotes electron donation, while oxidized forms contribute to nanoparticle stability and growth (Scampicchio *et al.*, 2006). Through chelation, caffeic and coumaric acids control nucleation and growth processes, forming well-defined nanoparticles, further stabilized by adsorbent bonds between phenolic acids' carboxyl groups and metal atoms (Nilsson *et al.*, 2008). Similarly, luteolin's enol form releases reactive hydrogen to convert silver ions (Ag^{+}) into elemental silver (Ag^{0}) (Muniyappan *et al.*, 2014), while quercetin chelates metal ions at multiple positions, aiding in adsorption on metal surfaces, nanoparticle formation, aggregation, and bioreduction (Makarov *et al.*, 2014). In blackberry fruit extract, flavonoids with hydroxyl and carbonyl groups adsorb on silver nanoparticles and take part in the reduction process (Kumar *et al.*, 2017). Mallikarjuna *et al.* (2014) highlighted the importance of pepper-derived leaf extracts rich in flavonoids and terpenoids for AgNPs bioreduction. Phytochemicals from *Ajuga bracteosa*, including flavonoids, terpenoids, ergosterol peroxide, and iridoid glycosides, prevent agglomeration during AgNPs synthesis, contributing to stability by providing spatial resistance and electrostatic repulsion (Afreen *et al.*, 2020; Kanniah *et al.*, 2021). Hence, the phytometabolites present in both plants serve as reducing agents, mediate nucleation and growth, and stabilize nanoparticles through surface interactions as given in Table 5. The absorption bands observed at various wavelengths can be linked to diverse electronic transitions of the phytochemicals within the leaf extracts, indicating the presence of phenolics, flavonoids, alkaloids, and tannins (Patel *et al.*, 2020). In *L. leucocephala*, caffeic acid is primarily characterized by absorption bands at 327, 297, 246, and 219 nm. The absorption at 297 and 219 nm is attributed to the $n\rightarrow\pi^*$ and $\pi\rightarrow\pi^*$ electronic transitions, respectively, associated with the C=O group. Additionally, the bands at 246 and 327 nm correspond to the $\pi\rightarrow\pi^*$ transitions of the aromatic moiety (Tošović, 2017). The absorbance intensity observed in the 190-400 nm range indicates the electronic transition of $n\rightarrow\pi^*$ in caffeic acid and chlorogenic acid molecules (Suhandy, 2017; Suhandy & Yulia, 2021). Previously reported UV-vis spectra of standard compounds, including gallic acid, quercetin, rutin, and tannic acid, confirm the presence of various compounds in plant extracts. Specific absorption bands at 265 nm for gallic acid, 250 nm and 370 nm for quercetin, 250 nm and 355 nm for rutin, and 275 nm for tannic acid indicate the presence of alkaloids, flavonoids,

phenolic acids, and tannins (Patle *et al.*, 2020). In our study, *A. oppositifolia* extracts exhibited similar absorption bands: 282 nm (gallic acid), 257 and 324 nm (quercetin), and 292 nm (tannic acid). In *L. leucocephala* extract, peaks at approximately 284 nm, 257 and 307 nm suggested the presence of gallic acid and quercetin, 297 nm indicating tannic acid. The presence of two absorption spectra for phenolic and flavonoid compounds can be attributed to the aromatic ring and other rings present in these compounds. Specifically, the absorption band observed at 280 nm and another in the range of 300-600 nm indicates π-π* transitions occurring within the aromatic system and transitions within other rings, respectively. Additionally, the appearance of a second broad band can be attributed to the overlapping with ligand to metal charge transfer bands (Vihakas, 2014; Hamad, 2012).

Phytometabolites	Role in Phytofabrication of AgNPs	Reference
Caffeic Acid	Acts as a reducing agent and stabilizer	(Guo *et al.*, 2015)
Chlorogenic Acid	Serves as a reducing agent and stabilizer	(Noh *et al.*, 2013)
Protocatechuic Acid	Functions as a reducing agent and stabilizer	(Noh *et al.*, 2013)
Coumaric Acid	Facilitates interaction between caffeic acid and iron, resulting in nanoparticle formation	(Nilsson *et al.*, 2008)
Ferulic Acid	Acts as a reducing agent	(Wang *et al.*, 2007)
Flavonoids	Adsorb onto the metal surface, interact with carbonyl groups or electrons, and are involved in the reduction process	(Kumar *et al.*, 2017)
Carotenoids and Terpenoids	Provide spatial resistance and electrostatic repulsion, thereby stabilizing the nanoparticles	(Mallikarjuna *et al.*, 2014) (Afreen *et al.*, 2020)

Table 5. Contributions of the phytometabolites in Green Synthesis of Silver Nanoparticles.

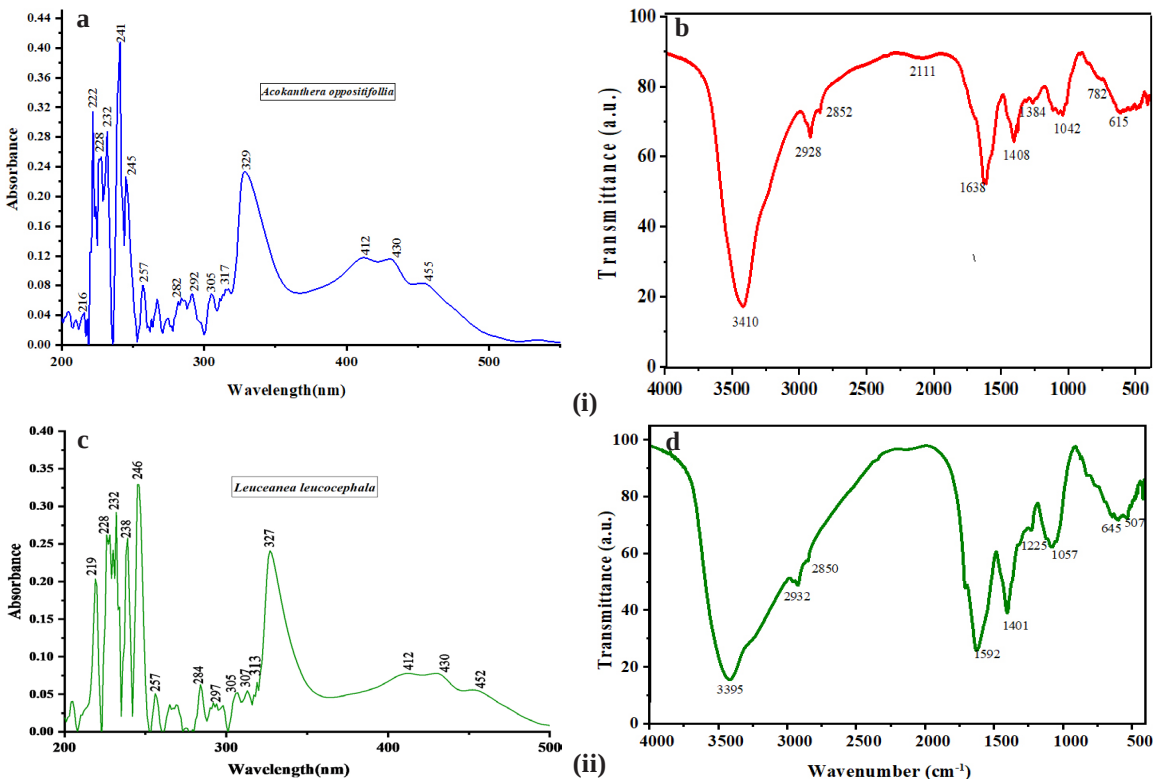

Figure 3. Uv-Visible and FTIR Spectroscopy profile of (i) *A. oppositifolia* and (ii) *L. leucocephala* aqueous extracts.

3.4. FTIR spectroscopy Analysis

FTIR spectral analysis of phytochemical compounds extracted from the leaves of both plants identified distinct functional groups that were categorized into six frequency ranges shown in Table 6. The remarkable peaks observed in Fig. 3b, d indicate the presence of various compounds: a broad and sharp peak at 3410 and 3395 cm^{-1} in *A. oppositifolia* and *L. leucocephala*, which corresponds to O-H bond stretching vibrations in alcohols and phenols, responsible for antioxidant activity in previous study (Sharma *et al*., 2015; Oliveira *et al*., 2016). Additionally peaks at 2928, 2852 and 2932, 2850 cm^{-1} indicate the presence of aliphatic compounds characterized by C-H bond stretching, which are common in alkanes. The presence of aliphatic compounds is further supported by the peak at 2111 cm^{-1} particularly in *A. oppositifolia*, which indicates the stretching vibration due to (C≡C) bonds typically associated with alkynes (Dhivya *et al*., 2017). The presence of primary and secondary amines and amides was confirmed by medium peaks at 1638 and 1592 cm^{-1} due to bending vibrations of the N-H bonds (Were *et al*., 2015). Other indicative peaks at 1418, 1384 and 1401 cm^{-1}, which are due to bending vibrations of the O-H bond, also support the presence of phenols or tertiary alcohols in aromatic compounds (Alara *et al*., 2018). Weak peaks at 1042, 1225 and 1057 cm^{-1} due to C–O bonds, indicating compounds such as alcohols, carboxylic acids, esters and ethers (Mabasa *et al*., 2021). Furthermore, weak peaks in the fingerprint region at 782, 615, 645 and 507 cm^{-1} indicate the stretching vibrations of C-X bonds found in alkyl halides of aliphatic compounds (Akinpelu *et al*., 2019). The FTIR spectrum suggest the presence of various functional groups that served as indicators for the presence of different phytochemical components present in both plants. The correlation between UV-vis and FTIR results reveals specific functional groups and compounds involved in reducing and stabilizing silver ions during AgNPs synthesis. UV spectra exhibit absorption maxima of various phytochemical compounds like phenols, flavonoids, and alkaloids, while FTIR spectra display corresponding functional groups. For example, in *A. oppositifolia* and *L. leucocephala*, O-H stretching vibrations in alcohols and phenols appear at 3410 cm^{-1} and 3395 cm^{-1}, respectively, and C-H stretching vibrations in alkanes were observed at 2928 cm^{-1}, 2852 cm^{-1}, and 2932 cm^{-1}, 2850 cm^{-1}. Additionally, C≡C stretching vibrations in alkynes was present at 2111 cm^{-1} in *A. oppositifolia*. Similarly, the peaks indicating the presence of phenols and flavonoids in the UV-vis spectra such as 282, 317 nm and 284, 313 nm correspond to peaks associated with O-H at 3410 cm^{-1} and 3395 cm^{-1} stretching and C-O stretching 1042 cm^{-1} and 1225 cm^{-1}, 1057 cm^{-1} in *A. oppositifolia* and *L. Leucocephala* respectively.

Frequency Range and Assigned group	Frequency peak		Chemical compounds
	A. oppositifolia	*L. leucocephala*	
3600-3200 (O-H stretch of Alcohols, phenols)	3410 (s)	3395 (s)	Aromatic
3000-2850 (C-H stretch of alkanes)	2928, 2852 (m)	2932, 2850 (m)	Aliphatic
2270-1940 (C≡C) stretch Alkyne	2111 (m-w)		Aliphatic
1640-1550 (N-H bending primary and secondary amines and amides)	1638 (m)	1592, (m)	Amines and amides
1410-1310 (O-H bend phenols or tertiary alcohol)	1418, 1384 (m)	1401 (m)	Aromatic
1320-1000 (C–O stretch Alcohols, carboxylic acids, esters, and ethers Acid and alcohol)	1042 (w)	1225, 1057 (w)	Acid and alcohol
840-600 (C–X) stretch Alkyl halides	782, 615 (w)	645, 507 (w)	Aliphatic

Table 6. FTIR spectral peak value and functional groups obtained for *A. oppositifolia* and *L. Leucocephala.* (s, m, w represents short, medium and weak).

The FTIR peaks at 3410 cm^{-1}, 1418 cm^{-1} and 3395 cm^{-1}, 1401 cm^{-1} and band at Uv-vis spectra 228 nm, 305 nm and 228 nm, 307 nm in *A. oppositifolia* and *L. leucocephala*, respectively, indicate the presence of p-Coumaric acid (Gao *et al.*, 2020). *L. leucocephala* exhibits two primary peaks at 3395 cm^{-1} and 1401 cm^{-1} for caffeic acid, while a narrow and intensive band between 3400-3300 cm^{-1} represents ferulic acid consistent with the UV-vis findings indicate the presence of both compounds (Dimitrić-Marković *et al.*, 2001). Moreover, spectra of chlorogenic and tannic acids display a broad and intensive band around 3400 cm^{-1} due to the hydrogen bond of the dimeric form of the acids. The FTIR spectrum of pure caffeic acid shows OH stretching vibrations between 4000-2600 cm^{-1}, partially overlapping with weak CH stretching modes (Catauro *et al.*, 2020). In the UV-vis spectra of *L. leucocephala*, absorption bands at 327 nm, 297 nm, 246 nm, and 219 nm characterize caffeic acid. The absorbance intensity in the 190-400 nm range suggests the electronic transition of $n \rightarrow \pi^*$ in caffeic acid and chlorogenic acid molecules, with a peak at 297 nm indicating tannic acid (Suhandy,2017; Suhandy & Yulia,2021). This correlation suggests that the phenols and flavonoids identified in the plant extracts are indeed responsible for the phytofabrication of nanoparticles.

3.5. Phytometabolite profiling by GCMS

The chromatogram of aqueous leaf extracts of both plants exhibited 23 different peaks related to bioactive compounds for *A. oppositifolia* and 15 different peaks for *L. leucocephala*. In *A. oppositifolia*, the major phytometabolites identified included Meadowlactone, A-Neooleana-3(5),12-diene, Boron,(1,3-butanediiminato-N,N')-1,5-cyclooctanediyl-,(t-4), 8-Isopropenyl-1,5-dimethylcyclodeca-1,5-diene, and Friedelan-3-one as depicted in Fig. 4a. For *L. leucocephala*, the identified phytometabolites were (1-(10,10-Dimethyl-3,3-dioxo-3-thia-4-azatricyclo (5.2.1.0 (1,5))dec-4-yl)-3-methylpent-4-en1-one, 3-(1H-benzimidazol-2-yl)-1-(4-(2,4-dimethylphenyl)-1 piperazinyl)-1-propanone, Boron (1,3-butanediiminato-N,N')-1,5-cyclooctanediyl-,(t-4)-, Lup-20(29)-en-3-one, and Friedelan-3-one as shown in Fig. 4b.

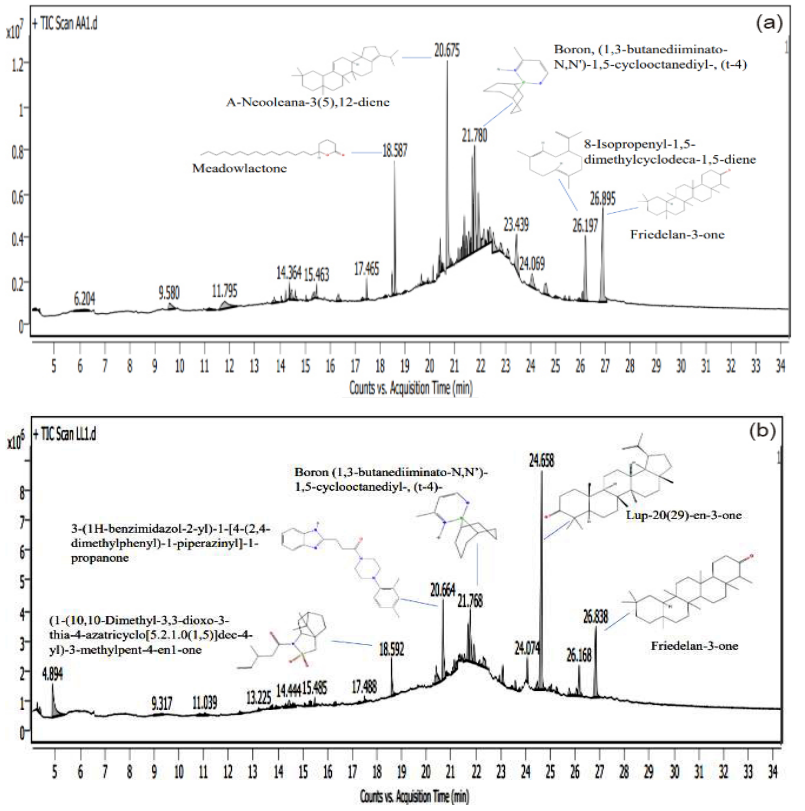

Figure 4. GCMS chromatogram of aqueous extracts for (a) *A. oppositifolia* and (b) *L. leucocephala.*

Some of the phytocompounds was found to be common in both the species of plants. These common compounds include Arsenic acid, tris(trimethylsilyl) ester, Heptasiloxane,1,1,3,3,5,5,7,7,9,9,11,11,13,13Tetradecamethyl-, Octasiloxane,1,1,3,3,5,5,7,7,9,9,11,11,13,13,15,15-hexadecamethyl, 3-(1H-Benzimidazol-2-yl)-1-(4-(2,4-dimethylphenyl)-1-piperazinyl)-1-propanone, Boron, (1,3-butanediiminato-N,N')-1,5-cyclooctanediyl-,(t-4), 4-Phosphacyclopentene, 4-mesityl, Friedelan-3-one. In previous studies these phytochemicals found to be responsible for several biological activities (Akinpelu *et al.*, 2019; Manikandan *et al.*, 2019). Such as Arsenous acid, tris(trimethylsilyl) ester, was found in methanolic extracts of *Momordica cymbalaria*, potentially useful in rheumatism, skin infections, diarrhea, diabetes and ulcers (Manikandan *et al.*, 2019). Furthermore, this compound was identified in *Gloriosa superba* Linn, which exhibits antioxidant activity (Singh *et al.*, 2023). Previous reports have indicated that Meadowlactone has the potential to improve skin and hair (Wohlman *et al.*, 2009). P. hydaspidis is thought to have anticancer properties due to the presence of meadowlactone (Ali *et al.*, 2021). A-neooleana-3(5),12-Diene, a type of terpenoid, has demonstrated anti-inflammatory, antimicrobial and antidiabetic properties (Wohlman *et al.*, 2009; Ali *et al.*, 2021). The compound 8-Isopropenyl-1,5-dimethylcyclodeca-1,5-diene found in ginger has shown an antibacterial effect (Sharif *et al.*, 2016). The antidiabetic properties of terpenoids like Friedelan-3-one have been previously documented and studied (Harley *et al.*, 2021; Rasyid *et al.*, 2023). The sea cucumber extracts showed both antibacterial and antioxidant effects, with cyclotetrasiloxane, octamethyl, identified as the main compound (Rasyid *et al.*, 2023). Similarly in papaya heptasiloxane,1,1,3,3,5,5,7,7,9,9,11,11,13,13-tetradecamethyl, was responsible for its insecticidal properties (Indramati *et al.*, 2023). Lup-20(29)-en-3-ol, acetate, (3β)- possess ability to inhibit tyrosinase and also showed anti-inflammatory, analgesic and antibacterial properties (Ahmed *et al.*, 2022; Malik *et al.*, 2017). The identification of A-neooleana-3(5),12-Diene, Friedelan-3-one, and Lup-20(29)-en-3-one as terpenoids in *L. leucocephala* contrasts with the presence of 9,19-Cyclolanost-24-en-3-ol, (3.beta.)-TMS derivative steroids, and 8-Isopropenyl-1,5-dimethylcyclodeca-1,5-diene, recognized as sesquiterpenoids, and Cyclodecacyclotetradecene, 14,15-didehydro1,4,5,8,9,10,11,12,13,16,17,18,19,20-tetradecahydro Diterpenoids in *A. oppositifolia*. Additionally, long-chain fatty acids such as Octasiloxane and Heptasiloxane are found in both plants (Ahmed *et al.*, 2022). This diversity of bioactive compounds is validated by consistent findings from UV-vis, FTIR, and TLC analyses conducted on both plant species.

3.6. Importance of these phytochemicals in nanoparticles synthesis

Phytochemicals extracted from plant leaves acted as reducing agents for silver nitrate under controlled conditions and produced stable AgNPs, as shown in Fig. 5 a, b. The resulting spherical AgNPs with 13.38 and 11.93 nm was produced from *A. oppositifolia* and *L. leucocephala*, as detailed in our previous research (Sharma *et al.*, 2023). TEM analysis revealed light-colored material on the surface, indicating nanoparticle capping by phytomolecules.

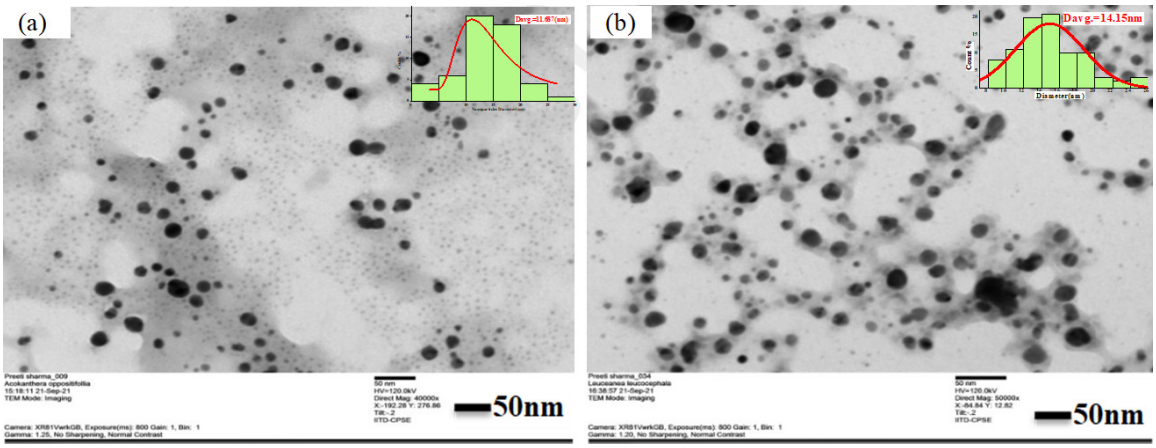

Figure 5. TEM micrographs of phytofabricated AgNPs from (a) *A. oppositifolia* and (b) *L. leucocephala*.

The UV-vis spectra of the AgNPs synthesized from the aqueous plant extracts indeed exhibited a shift in the absorption bands. Specifically, peaks were observed at 431 nm for *A. oppositifolia* and 436 nm for *L. leucocephala*, contrasting with the maximum absorbance at 287 nm observed in the aqueous form of $AgNO_3$ (Sharma *et al*., 2023). However, the aqueous extracts of both plants exhibited multiple peaks over a broad range of wavelengths, typically from 200 to 600 nm Fig. 3 a, c. These peaks represent the electronic transitions of various phytochemicals present in the extracts, such as alkaloids, phenols, flavonoids, and other metabolites. The presence of diverse functional groups, including carboxyl, hydroxyl, and amino groups, in these phytochemicals contributes to their unique absorption spectra. The absrbtion band with specific wavelengths indicating the $n\rightarrow\pi^*$ and $\pi\rightarrow\pi^*$ transitions occurring within the aromatic ring of phenolics, flavonoids, and alkaloids, as well as transitions within other rings present in these compounds as discussed earlier. On the other hand, the sharp peak reported in the 2023 paper for $AgNO_3$ synthesis suggests a more homogeneous population of nanoparticles with a well-defined size and shape. The silver nanoparticles involve the reduction of silver ions by a reducing agent, leading to the formation of nanoparticles with characteristic surface plasmon resonance (SPR) absorption peaks. Unlike the complex mixture of phytochemicals present in medicinal plant extracts, the synthesized nanoparticles exhibit a single SPR peak due to the collective oscillation of conduction electrons on the nanoparticle surface. Phytofabrication involves a more controlled process with specific reducing and stabilizing agents. Therefore, the difference in UV-vis absorption peaks between medicinal plants and $AgNO_3$ synthesis reflects the complex mixture of phytochemicals present in plant extracts versus the controlled synthesis conditions and specific chemical agents used in nanoparticle fabrication. The XRD peaks observed at 32.39° and 44.45° indicate the capping and stabilization of silver nanoparticles by plant metabolites. Additionally, certain unidentified peaks may be attributed to organic compounds derived from the plant extract, as elaborated in our prior study (Sharma *et al.,* 2023).The similarity of the FTIR spectra between functional nanoparticles and plant extracts indicates the presence of phytochemicals, while the observed changes being due to their involvement in the reduction process. EDX showed significant carbon and oxygen, confirming nanoparticle surface coating by phytochemicals. These results support the earlier study that highlighted the presence of phytochemicals coating the surface of nanoparticles (Yasmin *et al.,* 2014; Bykkam *et al*., 2015). Some phytometabolites on the surface have inherent reducing properties and promote silver reduction (Ag^+) for nanoparticle synthesis. Certain phytometabolites possess functional groups to stabilize nanoparticles and act as capping agents that control their size, shape and stability. The therapeutic properties of phytocompounds in the synthesized nanoparticles contribute to their biocompatibility, vital for potential biomedical applications, attributed to their previously reported antibacterial effectiveness of these synthesized nanoparticles (Sharma *et al.,* 2023). These phytometabolites may enhance the diverse properties (optical, magnetic, catalytic etc.) of the nanoparticles, making them suitable for various applications. For instance, these nanoparticles help in degrading Amoxicillin and have antimutagenic potential in water treatment and enable urea sensing in milk without using enzymes (Sharma *et al.,* 2023). Therefore, this study strongly suggests that the specific phytochemicals (phenols, flavonoids, alkaloids, carotenoids and terpenoids) found in aqueous extracts are crucial for the formation of silver nanoparticles formation.

4. CONCLUSION

This study demonstrates the diverse phytochemicals present in the extracts of *A. oppositifolia* and *L. leucocephala* which emphasizes the free phytochemicals play an important role in determining the overall phytochemical composition in plant extracts. This study leverages our previous research efforts in 2015 and 2023, to highlight the broader utility of medicinal plant extracts, particularly from *A. oppositifolia* and *L. leucocephala.* Our previous studies laid the foundation by exploring the potential applications of these extracts in nanotechnology, particularly in the synthesis and characterization of silver nanoparticles. Their therapeutic potential, effectiveness in wastewater treatment and catalytic properties, all due to the presence of these various phytometabolites as described earlier.Furthermore, our previous studies have pointed out the diverse potentials of these nanoparticles, ranging from antimicrobial activity to antimutagenic properties. In current study, we delve deeper into the phytochemical composition of these extracts and their role in the synthesis of stable silver nanoparticles.

The results confirm the effectiveness of these compounds, including phenols, flavonoids, alkaloids, carotenoids and terpenoids, as both reducing agents and stabilizers. These phytochemicals provide spatial resistance, electrostatic repulsion, and surface interactions to prevent agglomeration and stabilize the production of AgNPs.

By integrating our previous work with these new findings, we have advanced our understanding of environmental friendly silver nanoparticle synthesis using plant extracts. The abundant phenolic and flavonoid content in plant extracts from *A. oppositifolia* and *L. leucocephala* offers potential for the reduction of various metal ions, resulting in nanomaterials that can be used in medicine, catalysis, and environmental remediation. Expanding the phytofabrication approach to include metal oxide nanoparticles opens up opportunities to improve magnetic properties and photocatalysis, which are beneficial for wastewater treatment and solar cells. Furthermore, hybrid nanomaterials that integrate plant-derived carbon materials with metal nanoparticles exhibit improved properties for energy storage and sensing applications. Therefore, exploring phytofabrication in nanoformulations beyond silver nanoparticles can provide valuable insight for plant-based reduction process for various nanomaterials. This study marks a significant step towards sustainable nanotechnology with potential applications in various areas. Overall, this coherent presentation of research underlines the diverse benefits and versatility of medicinal plant extracts in nanotechnology.

Conflicts of Interest

The authors affirm that there are no conflicts of interest. ♦

REFERENCES

Adedapo, A. A., Jimoh, F. O., Afolayan, A. J., & Masika, P. J. (2008). Antioxidant activities and phenolic contents of the methanol extracts of the stems of Acokanthera oppositifolia and Adenia gummifera. *BMC Complementary and Alternative Medicine, 8*, 1-7. https://doi.org/10.1186/1472-6882-8-54

Adinortey, C. A., Kwarko, G. B., Koranteng, R., Boison, D., Obuaba, I., Wilson, M. D., & Kwofie, S. K. (2022). Molecular structure-based screening of the constituents of Calotropis procera identifies potential inhibitors of diabetes mellitus target alpha glucosidase. *Current Issues in Molecular Biology, 44*(2), 963-987. https://doi.org/10.3390/cimb44020064

Afreen, A., Ahmed, R., Mehboob, S., Tariq, M., Alghamdi, H. A., Zahid, A. A., … & Hasan, A. (2020). Phytochemical-assisted biosynthesis of silver nanoparticles from Ajuga bracteosa for biomedical applications. *Materials Research Express, 7*(7), 075404.DOI 10.1088/2053-1591/aba5d0

Ahmed, M., Khan, K. U. R., Ahmad, S., Aati, H. Y., Ovatlarnporn, C., Rehman, M. S. U., … & Anwar, M. (2022). Comprehensive phytochemical profiling, biological activities, and molecular docking studies of Pleurospermum candollei: An insight into potential for natural products development. *Molecules, 27*(13), 4113. https://doi.org/10.3390/molecules27134113

Ahsan, T., Li, B., Wu, Y., & Li, Z. (2023). Bio-Fabrication of ZnONPs from Alkalescent Nucleoside Antibiotic to Control Rice Blast: Impact on Pathogen (Magnaporthe grisea) and Host (Rice). *International Journal of Molecular Sciences, 24*(3), 2778.

Akinpelu, L. A., Olawuni, I. J., Ogundepo, G. E., Adegoke, A. M., Olayiwola, G., & Idowu, T. O. (2019). Spectroscopic analysis and anti-inflammatory effects of Milicia excelsa (Moraceae) leaf and fractions. *GSC Biological and Pharmaceutical Sciences, 6*(3), 051-060. https://doi.org/10.3390/ijms24032778

Alara, O. R., Abdurahman, N. H., Mudalip, S. K. A., & Olalere, O. A. (2018). Characterization and effect of extraction solvents on the yield and total phenolic content from Vernonia amygdalina leaves. *Journal of Food Measurement and Characterization, 12*, 311-316. https://doi.org/10.1007/s11694-017-9642-y

Aleixandre-Tudo, J. L., & Du Toit, W. (2018). The role of UV-visible spectroscopy for phenolic compounds quantification in winemaking. *Frontiers and new trends in the science of fermented food and beverages*, 200-204. DOI: 10.5772/intechopen.79550

Ali, S., Khan, M. R., Batool, R., Shah, S. A., Iqbal, J., Abbasi, B. A., … & Althobaiti, F. (2021). Characterization and phytochemical constituents of Periploca hydaspidis Falc crude extract and its anticancer activities. *Saudi Journal of Biological Sciences, 28*(10), 5500-5517. https://doi.org/10.1016/j.sjbs.2021.08.020

Alzandi, A. A., Taher, E. A., Al-Sagheer, N. A., Al-Khulaidi, A. W., Azizi, M., & Naguib, D. M. (2021). Phytochemical components, antioxidant and anticancer activity of 18 major medicinal plants in Albaha region, Saudi Arabia. *Biocatalysis and Agricultural Biotechnology*, *34*, 102020. https://doi.org/10.1016/j.bcab.2021.102020

Bachheti, A., Bachheti, R. K., Abate, L., & Husen, A. (2022). Current status of Aloe-based nanoparticle fabrication, characterization and their application in some cutting-edge areas. *South African Journal of Botany*, *147*, 1058-1069. https://doi.org/10.1016/j.sajb.2021.08.021

Bachheti, R. K., & Bachheti, A. (Eds.). (2023). Secondary Metabolites from Medicinal Plants: Nanoparticles Synthesis and Their Applications. *CRC Press*. https://doi.org/10.1201/9781003213727

Belay, A., & Gholap, A. V. (2009). Characterization and determination of chlorogenic acids (CGA) in coffee beans by UV-Vis spectroscopy. *African Journal of Pure and Applied Chemistry*, *3*(11), 234-240. http://www.academicjournals.org/ajpac

Bykkam, S., Ahmadipour, M., Narisngam, S., Kalagadda, V. R., & Chidurala, S. C. (2015). Extensive studies on X-ray diffraction of green synthesized silver nanoparticles. *Adv. Nanopart*, *4*(1), 1-10. http://dx.doi.org/10.4236/anp.2015.41001

Catauro, M., Barrino, F., Dal Poggetto, G., Crescente, G., Piccolella, S., & Pacifico, S. (2020). New SiO2/caffeic acid hybrid materials: Synthesis, spectroscopic characterization, and bioactivity. *Materials*, *13*(2), 394. https://doi.org/10.3390/ma13020394

Chandra, H., Kumari, P., Bontempi, E., & Yadav, S. (2020). Medicinal plants: Treasure trove for green synthesis of metallic nanoparticles and their biomedical applications. *Biocatalysis and Agricultural Biotechnology*, *24*, 101518. https://doi.org/10.1016/j.bcab.2020.101518

Dai, J., & Mumper, R. J. (2010). Plant phenolics: extraction, analysis and their antioxidant and anticancer properties. *Molecules*, *15*(10), 7313-7352. https://doi.org/10.3390/molecules15107313

DeFilipps, R. A., & Krupnick, G. A. (2018). The medicinal plants of Myanmar. *PhytoKeys*, (102), 1. https://doi.org/10.3897/phytokeys.102.24380

Deshmukh, S., Shrivastava, B., & Bhajipale, N. (2018). A Review on Acacia species of therapeutics importance. *International Journal of Pharmaceutical and Biological Science Archive*, 6(4), 24-34.

Dhivya, K., & Kalaichelvi, K. (2017). Screening of phytoconstituents, UV-VIS Spectrum and FTIR analysis of Micrococca mercurialis (L.) Benth. *International Journal of Herbal Medicine*, *5*(6), 40-44. https://www.florajournal.com/archives/2017/vol5issue6/PartA/6-4-2-168.pdf

Dimitrić-Marković, J. M., Mioč, U. B., Baranac, J., & Nedić, Z. P. (2001). A study of the IR spectra of the copigments of malvin chloride with organic acids. *Journal of the Serbian Chemical Society*, *66*(7), 451-462.

Durán, M., Silveira, C. P., & Durán, N. (2015). Catalytic role of traditional enzymes for biosynthesis of biogenic metallic nanoparticles: a mini-review. *IET Nanobiotechnology*, *9*(5), 314-323. https://doi.org/10.1049/iet-nbt.2014.0054

Edreva, A., Velikova, V., Tsonev, T., Dagnon, S., Gürel, A., Aktaş, L., & Gesheva, E. (2008). Stress-protective role of secondary metabolites: diversity of functions and mechanisms. *Gen Appl Plant Physiol*, *34*(1-2), 67-78.

El-Kemary, M., Ibrahim, E., A-Ajmi, F., Khalifa, S. A., Alanazi, A. D., & El-Seedi, H. R. (2016). Calendula officinalis-mediated biosynthesis of silver nanoparticles and their electrochemical and optical characterization. *International Journal of Electrochemical Science*, *11*(12), 10795-10805. https://doi.org/10.20964/2016.12.88

Gao, B., Chen, D., Gu, B., Wang, T., Wang, Z., Yang, Y., … & Wang, G. (2020). Facile and highly effective synthesis of nitrogen-doped graphene quantum dots as a fluorescent sensing probe for Cu2+ detection. *Current Applied Physics*, *20*(4), 538-544. https://doi.org/10.1016/j.cap.2020.01.018

Gomathi, D., Kalaiselvi, M., Ravikumar, G., Devaki, K., & Uma, C. (2015). GC-MS analysis of bioactive compounds from the whole plant ethanolic extract of Evolvulus alsinoides (L.) L. *Journal of Food Science and Technology*, *52*, 1212-1217. https://doi.org/10.1007/s13197-013-1105-9

Guo, D., Dou, D., Ge, L., Huang, Z., Wang, L., & Gu, N. (2015). A caffeic acid mediated facile synthesis of silver nanoparticles with powerful anti-cancer activity. *Colloids and Surfaces B: Biointerfaces*, *134*, 229-234. https://doi.org/10.1016/j.colsurfb.2015.06.070

Gururaja, K., & David, M. (2016). Spectroscopic signature, antibacterial and anticancer

properties of Calotropis gigantea (Linn.) flower. *International Journal of Pharmaceutical Sciences and Research, 7*(4), 1686. 10.13040/IJPSR.0975-8232.7(4).1686-93

Hamad, M. N. (2012). Isolation of rutin from Ruta graveolens (Rutaceae) cultivated in Iraq by precipitation and fractional solubilization. *Pharmacie Globale, 3*(4), 1.118717.

Harborne, A. J. (1998). *Phytochemical methods a guide to modern techniques of plant analysis*. Springer Science & Business Media.

Harley, B. K., Amponsah, I. K., Ben, I. O., Adongo, D. W., Mireku-Gyimah, N. A., Baah, M. K., … & Fleischer, T. C. (2021). Myrianthus libericus: Possible mechanisms of hypoglycaemic action and in silico prediction of pharmacokinetics and toxicity profile of its bioactive metabolite, friedelan-3-one. *Biomedicine & Pharmacotherapy, 137,* 111379. https://doi.org/10.1016/j.biopha.2021.111379

Hossain, M. A., AL-Raqmi, K. A. S., AL-Mijizy, Z. H., Weli, A. M., & Al-Riyami, Q. (2013). Study of total phenol, flavonoids contents and phytochemical screening of various leaves crude extracts of locally grown Thymus vulgaris. *Asian Pacific Journal of Ttropical Biomedicine, 3*(9), 705-710. https://doi.org/10.1016/S2221-1691(13)60142-2

Hussain, I., Singh, N. B., Singh, A., Singh, H., & Singh, S. C. (2016). Green synthesis of nanoparticles and its potential application. *Biotechnology Ltters, 38,* 545-560. https://doi.org/10.1007/s10529-015-2026-7

Ijaz, I., Gilani, E., Nazir, A., & Bukhari, A. (2020). Detail review on chemical, physical and green synthesis, classification, characterizations and applications of nanoparticles. *Green Chemistry Letters and Reviews, 13*(3), 223-245.https://doi.org/10.1080/17518253.2020.1802517

Indratmi, D., Haryanto, C. T., Rachmawan, M. D., & Zakia, A. (2023, May). Analysis of Volatile Metabolites from Papaya Seeds as Potential Organic Insecticides against Myzus persicae Sulz. In *IOP Conference Series: Earth and Environmental Science* (Vol. 1172, No. 1, p. 012046). IOP Publishing. DOI 10.1088/1755-1315/1172/1/012046

Kancherla, N., Dhakshinamoothi, A., Chitra, K., & Komaram, R. B. (2019). Preliminary analysis of phytoconstituents and evaluation of anthelminthic property of Cayratia auriculata (in vitro). *Maedica, 14*(4), 350. doi: 10.26574/maedica.2019.14.4.350

Kanniah, P., Chelliah, P., Thangapandi, J. R., Gnanadhas, G., Mahendran, V., & Robert, M. (2021). Green synthesis of antibacterial and cytotoxic silver nanoparticles by Piper nigrum seed extract and development of antibacterial silver based chitosan nanocomposite. *International Journal of Biological Macromolecules, 189,* 18-33. https://doi.org/10.1016/j.ijbiomac.2021.08.056

Kim, D. O., Jeong, S. W., & Lee, C. Y. (2003). Antioxidant capacity of phenolic phytochemicals from various cultivars of plums. *Food Chemistry, 81*(3), 321-326. https://doi.org/10.1016/S0308-8146(02)00423-5

Koul, A., Kumar, A., Singh, V. K., Tripathi, D. K., & Mallubhotla, S. (2018). Exploring plant-mediated copper, iron, titanium, and cerium oxide nanoparticles and their impacts. In *Nanomaterials in plants, algae, and microorganisms* (pp. 175-194). Academic Press. https://doi.org/10.1016/B978-0-12-811487-2.00008-6

Kowalski, R., & Kowalska, G. (2005). Phenolic acid contents in fruits of aubergine (Solanum melongena L.). *Polish Journal of Food and Nutrition Sciences, 14*(1), 37-41.

Krishna, A. B., Manikyam, H. K., Sharma, V. K., & Sharma, N. (2015). Plant cardenolides in therapeutics. *Int J Indigenous Med Plants, 48,* 1871-1896.

Kumar, B., Smita, K., Cumbal, L., & Debut, A. (2017). Green synthesis of silver nanoparticles using Andean blackberry fruit extract. *Saudi Journal of Biological Sciences, 24*(1), 45-50. https://doi.org/10.1016/j.sjbs.2015.09.006

Kurnia, E. D., Ratnasari, D., & Helmiawati, Y. (2019). Pembuatan Gel Ekstrak Daun Petai Cina (Leucaena glauca, Benth) Dengan Basis Gel Lidah (Aloe Vera L.) Buaya Sebagai Obat Luka Terbuka. *Journal of Holistic and Health Sciences (Jurnal Ilmu Holistik dan Kesehatan), 3*(1), 39-45.https://doi.org/10.51873/jhhs.v3i1.37

Lalrinzuali, K., Vabeiryureilai, M., & Jagetia, G. C. (2015). Phytochemical and TLC profiling of Oroxylum indicum and Milletia pachycarpa. *J Plant Biochem Physiol, 3*(152), 2. DOI: 10.4172/2329-9029.1000152

Mabasa, X. E., Mathomu, L. M., Madala, N. E., Musie, E. M., & Sigidi, M. T. (2021). Molecular spectroscopic (FTIR and UV-Vis) and hyphenated chromatographic (UHPLC-qTOF-MS) analysis and in vitro bioactivities of the Momordica balsamina leaf extract.

Biochemistry Research International, 2021. https://doi.org/10.1155/2021/2854217

Malik, W., Ahmed, D., & Izhar, S. (2017). Tyrosinase inhibitory activities of Carissa opaca Stapf ex haines roots extracts and their phytochemical analysis. *Pharmacognosy Magazine*, *13*(Suppl 3), S544. doi: 10.4103/pm.pm_561_16

Mallikarjuna, K., Sushma, N. J., Narasimha, G., Manoj, L., & Raju, B. D. P. (2014). Phytochemical fabrication and characterization of silver nanoparticles by using Pepper leaf broth. *Arabian Journal of Chemistry*, *7*(6), 1099-1103. https://doi.org/10.1016/j.arabjc.2012.04.001

Manikandan, G., Pandiselvi, P., Sobana, N., & Murugan, M. (2019). Gc-ms analysis of chemical constituents in the methanolic tuber extract of Momordica cymbalaria hook. *F. International Research Journal of Pharmacy.* 2019,10 (1). https://doi.org/10.7897/2230-8407.100122

Min, B., Gu, L., McClung, A. M., Bergman, C. J., & Chen, M. H. (2012). Free and bound total phenolic concentrations, antioxidant capacities, and profiles of proanthocyanidins and anthocyanins in whole grain rice (Oryza sativa L.) of different bran colours. *Food Chemistry*, *133*(3), 715-722. https://doi.org/10.1016/j.foodchem.2012.01.079

Muniyappan, N., & Nagarajan, N. S. (2014). Green synthesis of silver nanoparticles with Dalbergia spinosa leaves and their applications in biological and catalytic activities. *Process Biochemistry*, *49*(6), 1054-1061. https://doi.org/10.1016/j.procbio.2014.03.015

Nilsson, L., Lof, D., & Bergenståhl, B. (2008). Phenolic acid nanoparticle formation in iron-containing aqueous solutions. *Journal of Agricultural and Food Chemistry*, *56*(23), 11453-11457. https://doi.org/10.1021/jf8025925

Nistane, N. T., Chauriya, C. B., & Gajbhiye, V. R. (2019). A comparative pharmacognostic and antimicrobial evaluation of different parts of Mimusops elengi for dental associated problems. *Journal of Pharmacognosy and Phytochemistry*, *8*(4), 772-779. https://www.phytojournal.com/archives/2019/vol8issue4/PartN/8-3-651-110.pdf

Noh, H. J., Kim, H. S., Jun, S. H., Kang, Y. H., Cho, S., & Park, Y. (2013). Biogenic silver nanoparticles with chlorogenic acid as a bioreducing agent. *Journal of Nanoscience and Nanotechnology*, *13*(8), 5787-5793. https://doi.org/10.1166/jnn.2013.7492

Oliveira, R. N., Mancini, M. C., Oliveira, F. C. S. D., Passos, T. M., Quilty, B., Thiré, R. M. D. S. M., & McGuinness, G. B. (2016). FTIR analysis and quantification of phenols and flavonoids of five commercially available plants extracts used in wound healing. *Matéria (Rio de Janeiro)*, *21*, 767-779. https://doi.org/10.1590/S1517-707620160003.0072

Parlinska-Wojtan, M., Kus-Liskiewicz, M., Depciuch, J., & Sadik, O. (2016). Green synthesis and antibacterial effects of aqueous colloidal solutions of silver nanoparticles using camomile terpenoids as a combined reducing and capping agent. *Bioprocess and Biosystems Engineering*, *39*, 1213-1223. https://doi.org/10.1007/s00449-016-1599-4

Parry, E. (2007). Arrow poisons. *Zimbabwean Prehistory*, (27), 52-58.

Patle, T. K., Shrivas, K., Kurrey, R., Upadhyay, S., Jangde, R., & Chauhan, R. (2020). Phytochemical screening and determination of phenolics and flavonoids in Dillenia pentagyna using UV–vis and FTIR spectroscopy. Spectrochimica *Acta Part A: Molecular and Biomolecular Spectroscopy*, *242*, 118717. https://doi.org/10.1016/j.saa.2020.118717

Rasyid, A., & Putra, M. Y. (2023). Antibacterial and antioxidant activity of sea cucumber extracts collected from Lampung waters, *Indonesia. Kuwait Journal of Science*, *50*(4), 615-621. https://doi.org/10.1016/j.kjs.2023.03.012

Sanjivkumar, M., & Silambarasan, T. S. (2023). Exploration on Green Synthesis of Nanoparticles from Plants and Microorganisms and Their Biological Applications. In Modern Nanotechnology: Volume 2: Green Synthesis, Sustainable Energy and Impacts (pp. 149-173). *Cham: Springer Nature Switzerland.* https://doi.org/10.1007/978-3-031-31104-8_7

Saranraj, P., Sivasakthi, S., & Deepa, M. S. (2016). Phytochemistry of pharmacologically important medicinal plants – a review. *Int. J. Curr. Res. Chem. Pharm. Sci*, *3*(11), 56-66. DOI:10.22192/ijcrcps

Saxena, M., & Saxena, J. (2012). Evalution of phytoconstituents of Acorus calamus by FTIR and UV-VIS spectroscopic analysis. *International Journal of Biological & Pharmaceutical Research*, *3*(3), 498-501. https://www.phytojournal.com/archives/2016/vol5issue2/PartB/4-4-41.pdf

Scampicchio, M., Wang, J., Blasco, A. J., Sanchez Arribas, A., Mannino, S., & Escarpa, A. (2006). Nanoparticle-based assays of antioxidant

activity. *Analytical Chemistry*, *78*(6), 2060-2063. https://doi.org/10.1021/ac052007a

Shareef, H. K., Muhammed, H. J., Hussein, H. M., & Hameed, I. H. (2016). Antibacterial effect of ginger (Zingiber officinale) roscoe and bioactive chemical analysis using gas chromatography mass spectrum. *Oriental Journal of Chemistry*, *32*(2), 20-40. http://dx.doi.org/10.13005/ojc/320207

Sharma, P., & Chaurasia, S. (2015). Evaluation of total phenolic, flavonoid contents and antioxidant activity of Acokanthera oppositifolia and Leucaena leucocephala. *Int J Pharmacogn Phytochem Res*, *7*, 175-80. http://impactfactor.org/PDF/IJPPR/7/IJPPR,Vol7,Issue1,Article26.pdf

Sharma, P., & Sharma, B. (2023). Amoxicillin Degradation and Antimutagenic Potential of Phytofabricated Silver Nanoparticles-Doped Polyurethane Membrane for Wastewater Treatment. *Nano LIFE*, 2350009. https://doi.org/10.1142/S1793984423500095

Sharma, P., Sharma, B., Singh, I., & Kumari, P. (2023) Phytofabrication and characterization of silver nanoparticles and their enhanced antimicrobial activity. *Eurpoean Chemical Bulletin*, (12) 11. https://www.eurchembull.com/uploads/paper/33ba2caa1b0322ffb04f9ac4fc9b1b9a.pdf

Singh, A., Rai, G., Kumar, A., & Gautam, D. N. S. (2023). Pharmacognostical assessment, antioxidant ability and determination of phytomolecules using GC-MS in Gloriosa superba Linn. https://doi.org/10.21203/rs.3.rs-2620608/v1

Souto, U. T. D. C. P., Barbosa, M. F., Dantas, H. V., de Pontes, A. S., da Silva Lyra, W., Diniz, P. H. G. D., … & da Silva, E. C. (2015). Identification of adulteration in ground roasted coffees using UV–Vis spectroscopy and SPA-LDA. LWT-*Food Science and Technology*, *63*(2), 1037-1041. https://doi.org/10.1016/j.lwt.2015.04.003

Su, D., Zhang, R., Hou, F., Zhang, M., Guo, J., Huang, F., … & Wei, Z. (2014). Comparison of the free and bound phenolic profiles and cellular antioxidant activities of litchi pulp extracts from different solvents. *BMC Complementary and Alternative Medicine*, *14*, 1-10. https://doi.org/10.1186/1472-6882-14-9

Suhandy, D., & Yulia, M. (2017). Peaberry coffee discrimination using UV-visible spectroscopy combined with SIMCA and PLS-DA. *International Journal of Food Properties*, *20*(sup1), S331-S339. https://doi.org/10.1080/10942912.2017.1296861

Suhandy, D., & Yulia, M. (2018, October). The potential of UV-visible spectroscopy and chemometrics for determination of geographic origin of three specialty coffees in Indonesia. In *AIP Conference Proceedings* (Vol. 2021, No. 1). AIP Publishing. https://doi.org/10.1063/1.5062745

Tepal, P. (2016). Phytochemical screening, total flavonoid and phenolic content assays of various solvent extracts of tepal of Musa paradisiaca. *Malaysian Journal of Analytical Sciences,20*(5),1181-1190.DOI.ORG/10.1016/S2221-1691(13)60142-2

Tošović, J. (2017). Spectroscopic features of caffeic acid: theoretical study. *Kragujevac Journal of Science*, (39), 99-108.

Umashankar, D. D. (2020). Plant secondary metabolites as potential usage in regenerative medicine. *J. Phytopharmacol*, *9*(4), 270-273P. doi: 10.31254/phyto.2020.9410

Umboro, R. O., & Hamdani, A. S. (2019). Uji Daya Anthelmintik Ekstrak Etanol Biji Petai Cina (Leucaena leucocephala, Lmk. de Wit) terhadap cacing gelang (Ascaridia galli schrank) Secara In Vitro. *JISIP (Jurnal Ilmu Sosial dan Pendidikan)*, *3*(1). DOI: http://dx.doi.org/10.58258/jisip.v3i1.953

Vanitha, A., Kalimuthu, K., Chinnadurai, V., & Nisha, K. J. (2019). Phytochemical screening, FTIR and GC-MS analysis of aqueous extract of Caralluma bicolor – An endangered plant. *Asian J Pharm Pharmacol*, *5*(6), 1122-1130. DOI: 10.31024/ajpp.2019.5.6.7

Vihakas, M. (2014). *Flavonoids and other phenolic compounds: characterization and interactions with lepidopteran and sawfly larvae.*

Wang, H. Y., Li, Y. F., & Huang, C. Z. (2007). Detection of ferulic acid based on the plasmon resonance light scattering of silver nanoparticles. *Talanta*, *72*(5), 1698-1703. https://doi.org/10.1016/j.talanta.2007.02.028

Wang, L., Wei, G., Sun, L., Liu, Z., Song, Y., Yang, T., … & Li, Z. (2006). Self-assembly of cinnamic acid-capped gold nanoparticles. *Nanotechnology*, *17*(12), 2907.DOI 10.1088/0957-4484/17/12/014

Watt J. M. and Breyer-Brandwijk M. G. (1962). *The medicinal and poisonous plants of Southern and Eastern Africa*, 2nd edn. Livingstone, London, 15-18. 2

Were, P. S., Waudo, W., Ozwara, H. S., & Kutima, H. L. (2015). Phytochemical analysis of warburgia ugandensis sprague using fourier

transform infra-red (FT-IR) spectroscopy. International *Journal of Pharmacognosy and Phytochemical Research*, *7*(2), 201-205. http://impactfactor.org/PDF/IJPPR/7/IJPPR,Vol7,Issue2,Article1.pdf

Wohlman, A. (2009). Methods for enhancing the morphology, tone, texture and/or appearance of skin or hair using a meadowlactone." U.S. Patent 7,615,231. https://www.freepatentsonline.com/y2007/0092475.html

Yasmin, A., Ramesh, K., & Rajeshkumar, S. (2014). Optimization and stabilization of gold nanoparticles by using herbal plant extract with microwave heating. *Nano Convergence*, *1*(1), 12. https://doi.org/10.1186/s40580-014-0012-8

Yu, L., Haley, S., Perret, J., Harris, M., Wilson, J., & Qian, M. (2002). Free radical scavenging properties of wheat extracts. *Journal of Agricultural and Food Chemistry*, *50*(6), 1619-1624. https://doi.org/10.1021/jf010964p

Zhu, H., Liu, S., Yao, L., Wang, L., & Li, C. (2019). Free and bound phenolics of buckwheat varieties: HPLC characterization, antioxidant activity, and inhibitory potency towards α-glucosidase with molecular docking analysis. *Antioxidants*, *8*(12), 606.DOI: 10.3390/antiox8120606